Circulation Research

ORIGINAL RESEARCH

Macrophage-Expressed Coagulation Factor VII Promotes Adverse Cardiac Remodeling

Venkata Garlapati, Qi Luo,* Jens Posma,* Melania Aluia, Than Son Nguyen, Kristin Grunz, Michael Molitor, Stefanie Finger, Gregory Harms, Tobias Bopp, Wolfram Ruf, Philip Wenzel

BACKGROUND: Excess fibrotic remodeling causes cardiac dysfunction in ischemic heart disease, driven by MAP (mitogen-activated protein) kinase–dependent TGF-ß1 (transforming growth factor-ß1) activation by coagulation signaling of myeloid cells. How coagulation-inflammatory circuits can be specifically targeted to achieve beneficial macrophage reprogramming after myocardial infarction (MI) is not completely understood.

METHODS: Mice with permanent ligation of the left anterior descending artery were used to model nonreperfused MI and analyzed by single-cell RNA sequencing, protein expression changes, confocal microscopy, and longitudinal monitoring of recovery. We probed the role of the tissue factor (TF)-FVIIa (activated factor VII)-integrin ß1-PAR2 (protease-activated receptor 2) signaling complex by utilizing genetic mouse models and pharmacological intervention.

RESULTS: Cleavage-insensitive $PAR2^{R38E}$ and myeloid cell integrin ß1–deficient mice had improved cardiac function after MI compared with controls. Proximity ligation assays of monocytic cells demonstrated that colocalization of FVIIa with integrin ß1 was diminished in monocyte/macrophage FVII–deficient mice after MI. Compared with controls, $F7^{fl/fl}$ CX3CR1 (CX3C motif chemokine receptor 1)^{Cre} mice showed reduced TGF-ß1 and MAP kinase activation, as well as cardiac dysfunction after MI, despite unaltered overall recruitment of myeloid cells. Single-cell mRNA sequencing of CD45 (cluster of differentiation 45)$^+$ cells 3 and 7 days after MI uncovered a trajectory from recruited monocytes to inflammatory TF^+/TREM (triggered receptor expressed on myeloid cells) 1^+ macrophages requiring F7. As early as 7 days after MI, macrophage F7 deletion led to an expansion of reparative Olfml 3 (olfactomedin-like protein 3)$^+$ macrophages and, conversely, to a reduction of TF^+/$TREM1^+$ macrophages, which were also reduced in $PAR2^{R38E}$ mice. Short-term treatment from days 1 to 5 after nonreperfused MI with a monoclonal antibody inhibiting the macrophage TF-FVIIa-PAR2 signaling complex without anticoagulant activity improved cardiac dysfunction, decreased excess fibrosis, attenuated vascular endothelial dysfunction, and increased survival 28 days after MI.

CONCLUSIONS: Extravascular TF-FVIIa-PAR2 complex signaling drives inflammatory macrophage polarization in ischemic heart disease. Targeting this signaling complex for specific therapeutic macrophage reprogramming following MI attenuates cardiac fibrosis and improves cardiovascular function.

GRAPHIC ABSTRACT: A graphic abstract is available for this article.

Key Words: coagulation factors ■ fibrosis ■ heart failure ■ inflammation ■ macrophages ■ myocardial infarction

In This Issue, see p 803 | Meet the First Author, see p 804

Myocardial infarction (MI) remains a leading cause of death and disability worldwide, particularly when timely revascularization cannot be achieved. Persistent and subacute ischemia results in the development of ischemic heart failure, which is caused by tissue remodeling and excess cardiac fibrosis. Myeloid cells recruited to the ischemic myocardium play pivotal roles in repair and postischemic adverse remodeling.[1] Recruited

Correspondence to: Philip Wenzel, MD, Department of Cardiology and Center for Thrombosis and Hemostasis, University Medical Center Mainz, Langenbeckstr. 1, 55131 Mainz, Germany, Email wenzelp@uni-mainz.de; or Wolfram Ruf, MD, Center for Thrombosis and Hemostasis, University Medical Center Mainz, Langenbeckstr. 1, 55131 Mainz, Germany, Email ruf@uni-mainz.de
*Q. Luo and J. Posma contributed equally as shared second authors.
Supplemental Material is available at https://www.ahajournals.org/doi/suppl/10.1161/CIRCRESAHA.123.324114.
For Sources of Funding and Disclosures, see page 853.

Circulation Research is available at www.ahajournals.org/journal/res

ORIGINAL RESEARCH

Novelty and Significance

What Is Known?

- Anticoagulant and antiplatelet therapies are well-established in the management of ischemic heart disease.
- The tissue factor pathway plays a crucial role in mediating both inflammatory responses and tissue repair following acute injuries.

What New Information Does This Article Contribute?

- Novel role of macrophage-expressed factor VII in adverse postischemic cardiac remodeling.
- Interference with the noncoagulant functions of the TF-FVIIa complex rebalances macrophage functions from TREM (triggered receptor expressed on myeloid cells) 1 expressing inflammatory to TREM2$^+$ reparative macrophages after experimental myocardial infarction.
- Blockade of TF-FVIIa-PAR2 (protease-activated receptor 2) signaling pathway with a specific anti-TF antibody can improve long-term cardiovascular function without increasing bleeding risk.

Current treatments for ischemic heart disease include the inhibition of coagulation. However, these interventions often carry a high risk of bleeding. We here show that targeting the signaling properties of coagulation is sufficient to improve postischemic tissue repair after myocardial infarction modeled by permanent ligation of the left anterior descending artery. We delineate that the immune signaling functions of the coagulation initiation TF-FVIIa-PAR2 complex depend on the cell-autonomous synthesis of FVII and regulate macrophage polarization in ischemic cardiac tissue. Genetic ablation of the signaling functions or specific antibody inhibition of this complex induces a shift in injury-recruited monocyte differentiation from an inflammatory toward a reparative macrophage phenotype. These findings provide insight into a crucial myeloid cell intrinsic coagulation signaling pathway that determines ischemic remodeling after myocardial infarction and suggest potential new strategies for therapeutic intervention, particularly for patients with subacute and nonreperfused myocardial infarction who are at high risk to develop ischemic heart failure.

Nonstandard Abbreviations and Acronyms

Arg1	arginase 1
CCL2	C-C-motif chemokine ligand 2
CD45	cluster of differentiation 45
CD68	cluster of differentiation 68
CpG B	cytosine phosphate guanine B
Ctss	cathepsin S
CX3CR1	CX3C motif chemokine receptor 1
ERK	extracellular signal–regulated kinase
FX	factor X, encoded by the F10 gene
FVII	factor VII, encoded by the F7 gene
FVIIa	activated factor VII
FN1	fibronectin 1
IL	interleukin
Itgam	integrin alpha M
Itgb1	integrin beta 1
LAD	left anterior descending artery
LV	left ventricle
MAPK	mitogen-activated protein
MI	myocardial infarction
NAPc2	nematode anticoagulant protein c2
NOX	nicotinamide adenine dinucleotide phosphate hydrogen oxidase
Olfml3	olfactomedin-like protein 3
PAR2	protease-activated receptor 2
SMAD	mothers against decapentaplegic homolog
SPP1	secreted phosphoprotein 1
TF	tissue factor, encoded by the F3 gene
TGF-β1	transforming growth factor-β1
TLR-9	toll-like receptor 9
TREM	triggered receptor expressed on myeloid cells
WT	wild type

monocytes undergo spatiotemporal dynamic changes in the myocardium and differentiate into macrophages with distinct phenotypes. These can be precisely defined by their single-cell transcriptional profiles.[2–4] Several signaling pathways and receptors, including TREM (triggered receptor expressed on myeloid cells), have been implicated in the phenotypic differentiation of macrophages in regenerative processes and are linked to tissue homeostasis and repair in cardiac dysfunction.[2,5] Therapeutic immune interventions after MI have the potential to improve adverse remodeling, but preservation of host protective and reparative processes is of crucial importance for functional tissue repair.

Our previous study has uncovered a persistent complement and coagulation activation upstream of MAP

(mitogen-activated protein) kinase ERK (extracellular signal–regulated kinase) 1/2 phosphorylation in the myocardium of patients with chronic ischemic heart failure.[6] While thrombosis is an established trigger for acute cardiovascular events, continued activation of coagulation in cardiac tissue suggests roles of procoagulant pathways beyond acute atherothrombosis. Myeloid cells in the failing myocardium express the extrinsic coagulation initiator tissue factor (TF, encoded by the F3 gene), which is phosphorylated at its cytoplasmic domain, and the PAR2 (protease-activated receptor 2), which controls specifically the NOX (nicotinamide adenine dinucleotide phosphate hydrogen oxidase)2/ERK1/2-dependent activation of TGF-β1 (transforming growth factor-ß1) and profibrotic myofibroblasts. Genetic or pharmacological inhibition of the TF-PAR2-NOX2-ERK1/2-TGF-β1 pathway attenuates postischemic myocardial dysfunction and excess fibrosis.[6]

Here, we provide novel evidence that a cell-autonomous signaling pathway of monocyte-expressed factor VII (FVII, expressed by the F7 gene), the ligand for TF, is central for coagulation-inflammatory circuits in the infarcted myocardium and the differentiation of newly recruited monocytes into inflammatory macrophages. This signaling involves the association of the TF-FVIIa-PAR2 signaling complex with integrin adhesion receptors[7,8] and can be blocked with a specific anti-TF antibody with minimal antithrombotic activity.[9] The delineated monocyte reprogramming to yield a reparative immune cell phenotype could provide a therapeutic approach to achieve postischemic cardioprotection without an increased risk for bleeding complications.

METHODS

Data Availability

The data supporting the findings of this study can be obtained from the corresponding author upon reasonable request. Single-cell RNA sequencing data have been deposited in the Gene Expression Omnibus under the accession number GSE270768.

A detailed description of the methodology[10–25] is available in the Supplemental Material.

RESULTS

Proteolytic PAR2 Activation Is Linked to Myeloid Cell Integrin β1 Signaling Following MI

Because PAR2 is linked to different innate immune signaling pathways[6,11] and can be activated indirectly by heterodimeric PAR1/PAR2,[7] we first addressed the question of whether PAR2 proteolytic activation was required for pathological signaling in MI. We investigated mice with a point mutation of position 38 (arginine to glutamic acid) in the PAR2 extracellular domain that renders PAR2 cleavage resistant and insensitive to TF-FVIIa–mediated signal transduction (Figure 1A).[8] $PAR2^{R38E}$ mice were subjected to permanent left anterior descending artery (LAD) ligation to model nonreperfused MI; sham surgery was used as an additional control. Compared with strain-matched PAR2 wild-type (WT) controls, $PAR2^{R38E}$ mice had better left ventricle (LV) systolic function, indicating partial protection from MI-induced cardiac dysfunction despite having PAR2 protein expression comparable to controls (Figure 1B; Figure S1A). Thus, the previously shown profibrotic role of myeloid cell PAR2 in the development of ischemic heart failure requires the direct proteolytic activation of this receptor.

TF-FVIIa activates PAR2 by recruiting different receptor complexes, and integrin ß1 heterodimers especially support direct cleavage-dependent signaling of PAR2 downstream of TF-FVIIa supporting ERK1/2 activation.[8] On macrophages, TF-FVIIa traffics with integrin α4/β1 and TF-FVIIa regulates monocyte/macrophage migration on fibronectin, the extracellular matrix ligand for integrin α4/β1 and integrin α5/β1, in the context of nucleic acid sensing in inflammation.[9] While complete integrin ß1 (encoded by the Itgb1 gene) deficiency is embryonically lethal, deletion of Itgb1 in macrophage is permissive with development but prevents TF-dependent endosomal activation of the NOX2 in antiphospholipid antibody signaling.[7] Because TF also couples to NOX2 in adverse cardiac remodeling after MI,[6] we compared $Itgb1^{fl/fl}$ littermate controls with $Itgb1^{fl/fl}$ LysM (lysozyme M)^{Cre} mice after LAD ligation (Figure 1A). Myeloid cell integrin ß1–deficient mice had better LV systolic function and decreased left ventricular end diastolic volume, consistent with partial protection from adverse cardiac remodeling (Figure 1C).

Activation of TGF-ß1 and phosphorylation of downstream SMAD (mothers against decapentaplegic homolog) 2 were attenuated in the infarcted cardiac tissue of integrin ß1 floxed ($Itgb1^{fl/fl}$) $LysM^{Cre}$ mice relative to $Itgb1^{fl/fl}$ littermate controls 7 days after MI (Figure 1D). The number of myeloid cells accumulating in the infarcted myocardium was reduced 7 days after LAD ligation in myeloid cell integrin ß1–deficient mice but not altered 3 days after MI (Figure 1E; Figure S1B). This was paralleled by comparable expression of IL (interleukin)-6 and CCL2 (C-C-motif chemokine ligand 2) at day 3, indicating that the cardiac inflammatory milieu provoked by MI was not different between the 2 strains (Figure S1C). Importantly, TGF-ß1 activation started to decrease already at day 3, whereas myofibroblast activation indicated by p-SMAD2 was not yet altered in the infarcted myocardium (Figure S1D). These data suggest that myeloid cell integrin ß1 signaling is dispensable for the initial monocyte recruitment but plays a role in the subsequent differentiation and functional maturation of monocyte-derived macrophages in the specific coagulation-inflammatory tissue milieu of postischemic remodeling.

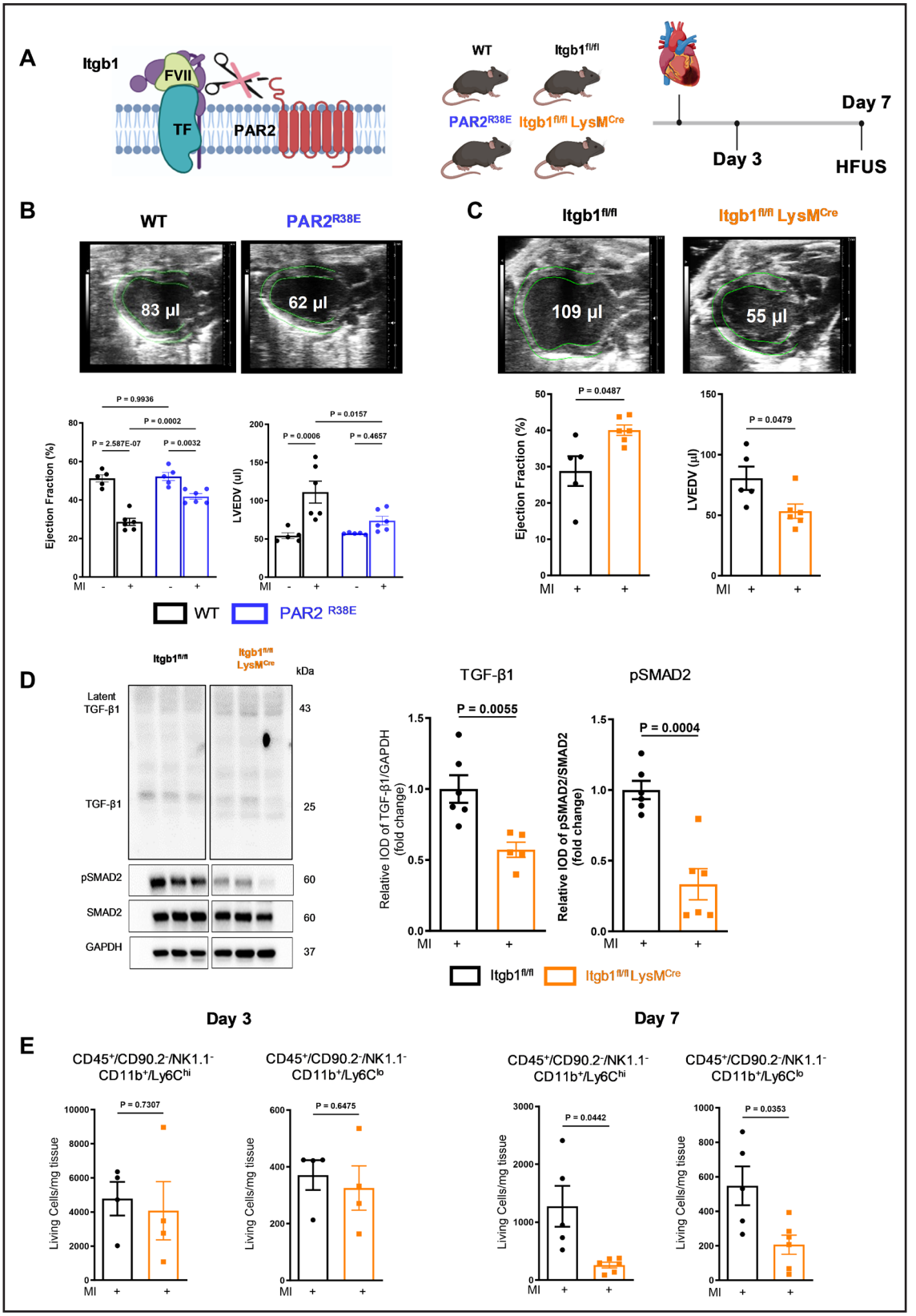

Figure 1. Myeloid cell integrin ß1 is linked to PAR2 (protease-activated receptor 2) cleavage–dependent cardiac dysfunction post-myocardial infarction (MI).

A, PAR2^{R38E} cleavage–insensitive and strain-matched control wild-type (WT) PAR2 mice were subjected to permanent left anterior descending artery (LAD) ligation. **B**, High-frequency ultrasound echocardiography (HFUS) 7 days after MI with quantification of left ventricular ejection fraction (LVEF) and left ventricular end diastolic volume (LVEDV). Mean±SEM; n=5 to 6 animals/group, 1-way ANOVA, Sidak (*Continued*)

Monocyte/Macrophage-Expressed FVII Promotes Adverse Remodeling After MI

The remarkable cardiac protection of myeloid cell integrin ß1–deficient mice indicated that myeloid cell integrin ß1 signaling supports TF-FVIIa signaling during ischemic remodeling following MI.[6] Although FVII in the blood is primarily synthesized in the liver, there is increasing evidence that extrahepatic synthesis of F7 by macrophages contributes to adaptive and inflammatory processes.[9,26,27] We, therefore, hypothesized that potential signaling connections between TF and integrin ß1 required the extrahepatic synthesis of FVII by monocytes/macrophages. We deleted F7 with the monocyte/macrophage-specific CX3CR1 (CX3C motif chemokine receptor 1)^{Cre} driver to create a deficiency of FVII in the monocytic lineage (Figure 2A). After permanent LAD ligation, FVII colocalized with integrin ß1 based on proximity ligation assay specifically in the infarcted tissue. Proximity was significantly reduced in F7$^{fl/fl}$ CX3CR1^{Cre} mice versus F7$^{fl/fl}$ littermate controls (Figure 2B). These data indicated that FVII associated with immune cells in the ischemic myocardium was derived at least in part from cell-autonomous synthesis by monocytes/macrophages.

Compared with littermate F7$^{fl/fl}$ controls, LAD-ligated F7$^{fl/fl}$ CX3CR1^{Cre} mice showed improved post-MI cardiac function and reduced LV dilatation (Figure 2C). This was paralleled by attenuation of MAPK (mitogen-activated protein) ERK1/2 phosphorylation, profibrotic TGF-ß1 activation, and downstream SMAD2 phosphorylation, a marker of fibroblast activation (Figure 2D). As seen with Itgb1$^{fl/fl}$ LysM^{Cre} mice, the abundance of accumulating immune cells in the infarcted tissue 3 days after MI did not differ between controls and monocyte/macrophage F7–deficient mice (Figure S2A). Remarkably, immune cell numbers and inflammatory markers (Figure S2B) in the infarcted myocardium were also similar between monocyte/macrophage F7–deficient mice and littermate WT controls 7 days after MI, suggesting that FVII specifically fine-tuned the macrophage phenotype for adverse remodeling.

We capitalized on the quantitatively similar numbers of infiltrating immune cells to characterize the FVII-induced phenotypic changes in monocytes/macrophages by single-cell RNA sequencing. We isolated CD45 (cluster of differentiation 45)$^+$ immune cells from the infarcted myocardium of littermate F7$^{fl/fl}$ and F7$^{fl/fl}$ CX3CR1^{Cre} mice 3 and 7 days after permanent LAD ligation. Unsupervised clustering of the merged data set showed that most retrieved cells were of the monocyte/macrophage lineage with few granulocytes, T cells, and contaminating stromal cells being captured (Figure S3A and S3B). Reclustering of monocyte/macrophage populations yielded 10 distinct clusters populated (Figure S3C) with different amounts of cells isolated from day 3 and 7 samples after LAD ligation (Figure S3D and S3E). Most clusters coexpressed F7 and CX3CR1 and showed reduced F7 levels in F7$^{fl/fl}$ CX3CR1^{Cre} relative to F7$^{fl/fl}$ control mice (Figure S3F).

This initial analysis was consistent with prior studies indicating that newly recruited monocytes differentiated into macrophages during myocardial remodeling after MI.[18] To further analyze the differentiation path, we enriched our data obtained on days 3 and 7 after MI by merging publicly available data sets[18] for CD45$^+$ myocardial cells at steady state and days 1, 5, and 7 (Figure 3A). This merging of data yielded an integrated Uniform Manifold Approximation and Projection (UMAP) with 13 clusters (Figure 3B) that were characterized by distinct expression profiles (Figure S4). The abundance of cells in these clusters differed between F7$^{fl/fl}$ CX3CR1^{Cre} and F7$^{fl/f}$ control mice, specifically on day 7 (Figure 3C). Clusters 6 and 10, which had an expression profile consistent with newly recruited monocytes (Figure S4), were most abundant on day 3. Comparison of the expression profiles of clusters 10 versus 6 showed an upregulation of macrophage maturity markers related to antigen presentation and regulation of adaptive immune responses (Figure S5A and S5B), suggesting sequential differentiation from clusters 6 to 10. At day 3, cell numbers in these clusters did not differ between monocyte F7–deficient and control mice, in line with the flow cytometry data (Figure S2A). Clusters 1, 11, and 12 also had similar cell numbers in both strains on day 3, but cell numbers within these clusters increased on day 7. Moreover, the abundance of cells in clusters 1, 11, and 12 cells sharing a more anti-inflammatory signature (Figure S4) was higher in F7$^{fl/fl}$ CX3CR1^{Cre} than in control mice 7 days post-MI. In contrast, more proinflammatory Arg1 (arginase 1)$^+$ macrophages in cluster 3 (Figure S4) increased in numbers in controls from day 3 to day 7 but remained unchanged in F7$^{fl/fl}$ CX3CR1^{Cre} mice (Figure 3C).

We next performed a trajectory analysis of monocyte differentiation in this merged data set. We uncovered

Figure 1 Continued. multiple comparison test. **C**, Integrin ß1 floxed (Itgb1$^{fl/fl}$) and myeloid cell integrin ß1–deficient Itgb1$^{fl/fl}$ LysM (lysozyme M)^{Cre} littermates were subjected to permanent LAD ligation and analyzed after 3 and 7 days. **C**, HFUS obtained from Itgb1$^{fl/fl}$ and Itgb1$^{fl/fl}$ LysM^{Cre} mice 7 days after MI with measurement of LVEF and LVEDV. Mean±SEM; n=5 to 6 animals/group, 1-way ANOVA, Sidak multiple comparison test. **D**, Protein expression analysis of TGF-β1 (transforming growth factor-ß1; normalized to GAPDH) and p-SMAD (mothers against decapentaplegic homolog) 2 (normalized to total SMAD2) in the infarcted myocardium. Representative blots and quantification of biological replicates. Mean±SEM, n=6 animals/group; Welch unpaired *t* test. **E**, Flow cytometry analysis of the infarcted myocardium obtained 3 and 7 days post-MI. Quantification of CD45 (cluster of differentiation 45)$^+$/CD90.2$^-$/B220$^-$/NK1.1 (killer cell lectin-like receptor subfamily B member 1C)$^-$/CD11b$^+$/Ly-6C (lymphocyte antigen 6 family member C)^{hi} monocytes and CD45$^+$/CD90.2$^-$/B220$^-$/NK1.1$^-$/CD11b$^+$/Ly-6C^{lo} macrophages. Mean±SEM, n=4 to 6 animals/group; Welch unpaired *t* test. Scheme created with the help of *BioRender*.com.

ORIGINAL RESEARCH

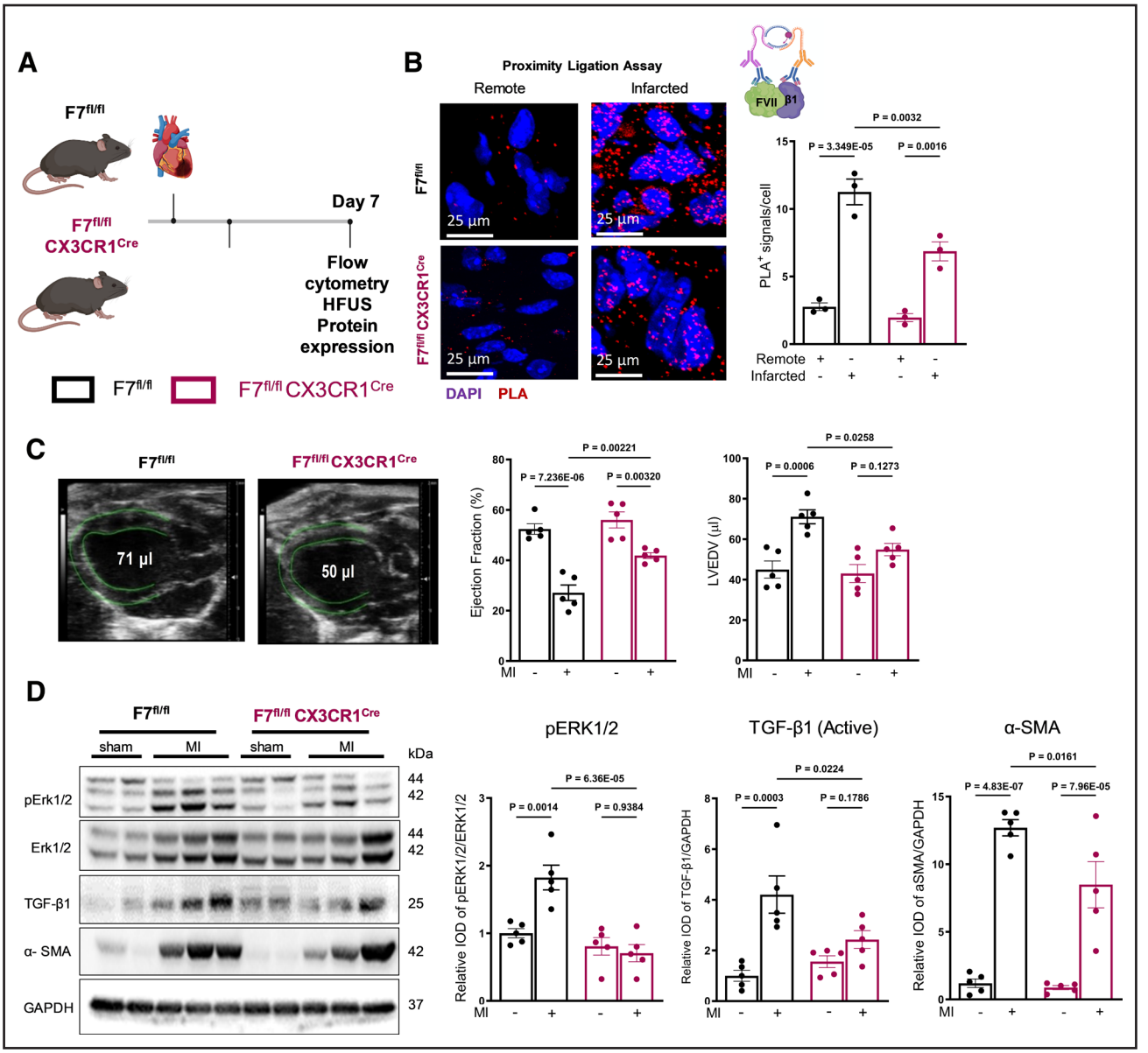

Figure 2. Monocyte-expressed factor VII (FVII) is required for pERK (extracellular signal–regulated kinase) 1/2 and TGF-β1 (transforming growth factor-ß1) activation and development of cardiac dysfunction after myocardial infarction (MI).
A, $F7^{fl/fl}$ and $F7^{fl/fl}$ CX3CR1 (CX3C motif chemokine receptor 1)^{Cre} littermates were subjected to permanent left anterior descending artery (LAD) ligation and investigated after 7 days. **B**, Proximity ligation assay (PLA) with red fluorescence spots for FVII and ITGB1 proximity in the infarcted and remote myocardium was measured 7 days post-MI with a 63× 1.4 numerical aperture (NA) oil immersion objective with sequential detection for 4′,6-diamidino-2-phenylindole (DAPI) and Alexa Fluor 594. n=3 animals/group; 1-way ANOVA, Sidak multiple comparison test. **C**, Assessment of cardiac function by high-frequency ultrasound 7 days after MI with quantification of left ventricular ejection fraction (LVEF) and left ventricular end diastolic volume (LVEDV). Mean±SEM, n=5 animals/group; 1-way ANOVA, Sidak multiple comparison test. **D**, Protein expression analysis and quantification of pERK1/2 (normalized to total ERK1/2), activated TGF-β1, and αSMA (alpha smooth muscle actin; normalized to GAPDH) at day 7. Mean±SEM, n=5 animals/group; 1-way ANOVA, Sidak multiple comparison test. Scheme created with the help of *BioRender*.com.

trajectories from early recruited monocytes in cluster 6 to proinflammatory monocytes in cluster 3 as opposed to a trajectory sequentially through clusters 12 and 11 to cluster 1 (Figure 3D). A differentiation path along clusters 9 and 8 to a monocyte-derived dendritic cell population in cluster 4 was also revealed in this analysis. Cluster 4 cell abundance neither changed from days 3 to 7 nor differed between WT and myeloid cell F7–deleted mice. While factor 10 (F10) was expressed in the newly recruited monocyte cluster 6, its expression peaked in cluster 10 and then remained relatively higher on the trajectory to cluster 3 compared with the alternative trajectory to cluster 1 (Figure 3E). In contrast, F7 mRNA expression increased along the trajectory to cluster 3, which was also characterized by high expression of the FVII receptor TF (encoded by F3 gene), indicating cell-autonomous synthesis and signaling of the TF-FVIIa complex. In addition, Arg1 and IL1a increased along

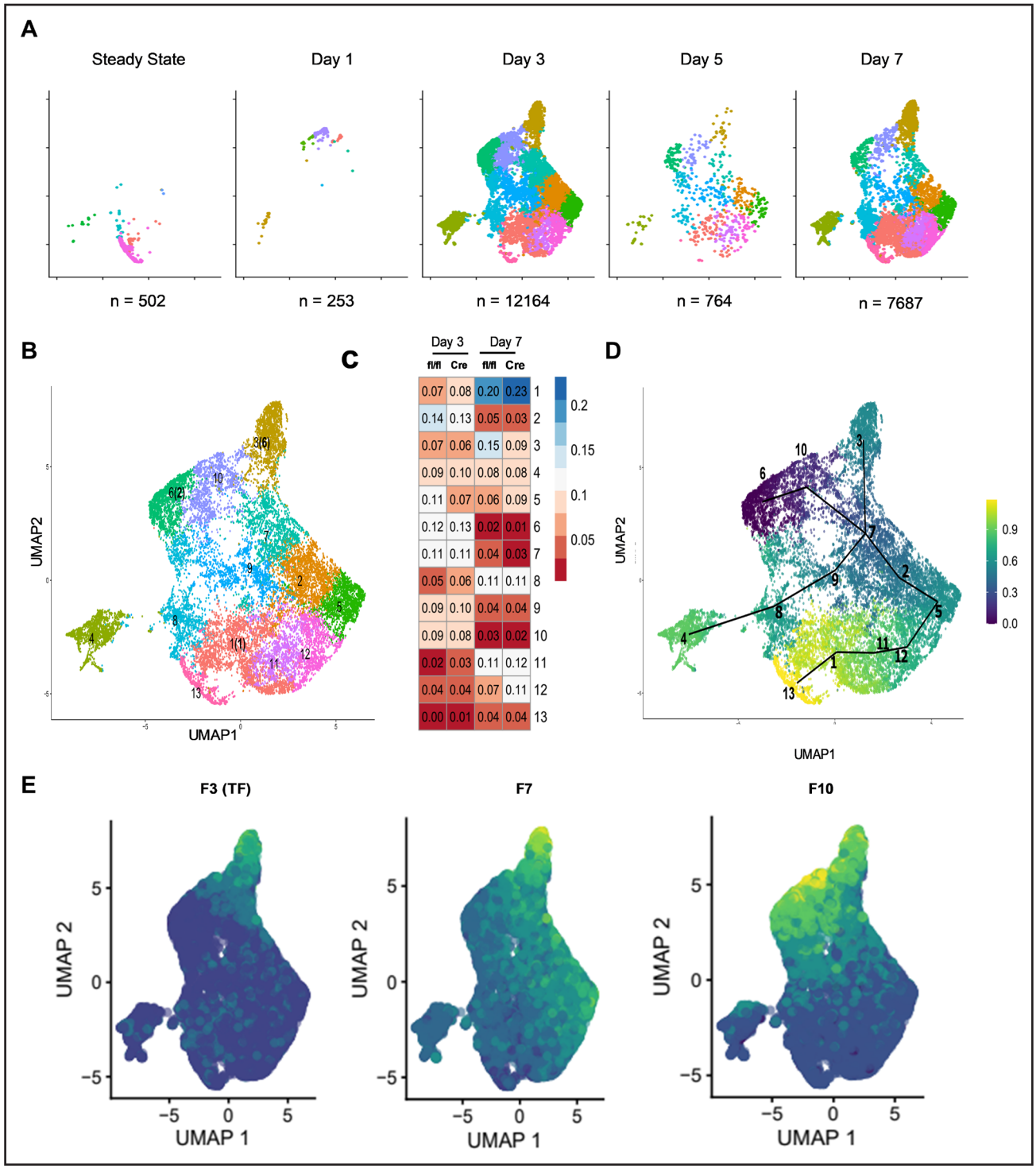

Figure 3. Single-cell sequencing of immune cells in the infarcted myocardium.
A, CD45 (cluster of differentiation 45)$^{+}$ single-cell data sets published by Haghverdi et al[19] (steady state before myocardial infarction [MI], days 1, 3, 5, and 7 post-MI) was integrated with our data set from days 3 and 7 post-MI obtained from 18 mice (day 3: factor 7 [F7]$^{fl/fl}$ mice: n=4; F7$^{fl/fl}$ CX3CR1 (CX3C motif chemokine receptor 1)^{Cre} mice: n=3; day 7: F7$^{fl/fl}$ mice: n=6; F7$^{fl/fl}$ CX3CR1^{Cre} mice: n=5) using the Fastmnn from the Batchelor package in R. Uniform Manifold Approximation and Projection (UMAP) plots and number of monocytic cell extracted from the integrated data sets at the different timepoints. **B**, Cluster numbering of the integrated data set. Corresponding clusters of the UMAP plots from Figure S2C are given in brackets. n=21 644 cells. **C**, Relative abundance of monocytic cells in clusters 1 to 13 in F7$^{fl/fl}$ and F7$^{fl/fl}$ CX3CR1^{cre} at days 3 and 7 in our data sets. **D**, Cells were positioned along a pseudotime trajectory path using the TSCAN package in R and color labeled according to their pseudotime. Cluster 6, the Ly6C2 (lymphocyte antigen 6 family member C)^{high} monocytes, was selected as the root of the trajectory. The minimum spanning tree trajectory path was visualized on top of the UMAP plot. **E**, mRNA Expression of tissue factor (TF; factor 3 [F3]), F7, and factor 10 (F10) along the trajectory in the UMAP plot.

the trajectory from cluster 6 to cluster 3 but decreased along the differentiation path to cluster 1. Conversely, transcripts increasing on the trajectory to cluster 1 (Ctss [cathepsin S] and lymphocyte granule membrane) remained unchanged or decreased on the trajectory to cluster 3 (Figure S6A and S6B).

Comparison of the expression profiles of cluster 3 with the combined data of early recruited monocytes/macrophages in clusters 6 and 10 revealed an upregulation of cell migration and immune activation pathways (Figure S7A and S7B). To identify relevant macrophage subpopulations in which TF-FVIIa might interact with integrin β1, we analyzed integrin expression of MI-recruited monocyte/macrophages. Violin plots of log-normalized counts of relevant integrin subunits showed that integrin αM/β2 was already expressed in the newly recruited monocyte/macrophage population in cluster 6 and markedly increased on the trajectory through cluster 10 to the detrimental macrophage population in cluster 3 expressing high levels of F3 and F7 (Figure 4A; Figure S8A). In contrast, integrin β1 was expressed at low levels by newly recruited monocyte/macrophages (cluster 6) but reached the highest level of expression in the detrimental F3/F7 expressing macrophages in cluster 3 (Figure 4A). In addition, integrin α subunits previously implicated in the interaction with TF-FVIIa[8] were also expressed by this macrophage phenotype (Figure S8B). Taken together, these data showed that the proinflammatory cluster 3 had the highest expression levels of not only F3 and F7 but also Itgb1 compared with all other clusters, including the reparative clusters 1, 11, and 12.

In addition to the expression of F3, F7, and F10, a comparison of cluster 3 with clusters 1, 11, and 12 identified TREM1 as a transcript characteristic for these CD68 (cluster of differentiation 68)$^+$ macrophages found at day 7 predominantly in WT mice. Additional transcripts discriminating CD68$^+$ cells between cluster 3 and clusters 1, 11, and 12, which shared a high degree of similarity, were the expression of TREM2 and of Olfml (olfactomedin-like protein) 3 (Figure 4B). Analysis of gene ontology terms characterizing cluster 3 versus the combined clusters 1, 11, and 12 showed that the latter had a tissue-homeostatic/reparative expression profile, whereas cluster 3 showed an inflammatory signature and patterns of leukocyte and ERK activation (Figure S9A), known to be implicated in profibrotic remodeling after MI.[6] Further analysis with an alternative bioinformatics pipeline confirmed that cluster 3 cells had a more inflammatory phenotype as opposed to cluster 1, 11, and 12 cells, which showed enrichment of pathways involved in homeostatic functions of macrophages (Figure 4C; Figure S9B).

To clarify the phenotypic changes of macrophage abundance in the spatial context of the infarcted myocardium, we analyzed the cellular distribution of the identified markers by immunohistochemistry in cardiac sections from mice 7 days after LAD ligation. Confocal microscopy showed that the CD68$^+$ macrophages were predominantly localized to the infarcted myocardium (Figure S10A through S10C), but the abundance of CD68$^+$ cells did not differ between F7$^{fl/fl}$ CX3CR1^{Cre} and littermate controls mice (Figure S10D). In contrast and in line with the single-cell transcriptomic data, CD68$^+$ macrophages double positive for TF or TREM1 were lower, whereas the number of CD68$^+$ Olfml3$^+$ cells was higher in F7$^{fl/fl}$ CX3CR1^{Cre} relative to F7$^{fl/fl}$ littermate controls (Figure 5A and 5B). We corroborated these results by investigating cardiac sections of LAD-ligated PAR2^{R38E} mice 7 days after MI (Figure S11A and S11B). PAR2^{R38E} mice had similar numbers of CD68$^+$ cells in the infarcted myocardium and phenocopied the F7$^{fl/fl}$ CX3CR1^{Cre} mice by a shift to a lower abundance of CD68$^+$TF$^+$ and CD68$^+$TREM1$^+$ macrophages relative to controls (Figure 5C and 5D). Western blotting also confirmed the overall reduced levels of TREM1 in the infarcted myocardium of PAR2^{R38E} relative to WT mice (Figure S11C). Thus, proteolytic TF-FVIIa-PAR2 signaling by monocyte/macrophages is a driver for the expansion of a more proinflammatory macrophage population during adverse remodeling after MI.

Inhibition of the TF-FVIIa Complex Preserves Cardiovascular Function After MI

Monoclonal antibodies can inhibit the integrin-dependent function of TF-FVIIa in cell signaling with minimal interference in TF-dependent coagulation.[8,9] Recently, a monoclonal antibody (43D8) to mouse TF without appreciable anticoagulant activity has been developed.[9] We evaluated anti-mouse TF 43D8 in a clotting assay initiated with mouse TF$^+$ cells. The function-blocking anti-mouse TF 21E10[25] was used as positive control and markedly prolonged clotting times relative to control IgG from 12.0±0.1 s to 39.5±1.7 s (P<0.0001), whereas the clotting time was not significantly prolonged by anti-mouse TF 43D8 (13.3±0.1 s). We next analyzed the effects of anti-mouse TF 43D8 on TF-FVIIa-PAR2 signaling–dependent macrophage migration stimulated by nucleic acid sensing,[9] which plays a pivotal role in the macrophage response to myocardial ischemia.[28] Considering our scRNA sequencing results revealing Itgb1$^+$ and Itgam$^+$ (integrin alpha M)/Itgb2$^+$ (integrin beta 2) cells in cluster 3, we stimulated macrophages with the DNA mimic and TLR-9 (toll-like receptor 9) activator CpG B (cytosine phosphate guanine B) and compared anti-mouse TF 43D8 to control IgG. CpG B–activated cells migrated more efficiently on the integrin β1 matrix fibronectin and the integrin αM/β2 matrix fibrin(ogen), but only the latter was inhibited by the signaling blocking anti-TF 43D8 compared with control IgG (Figure S12A). These data demonstrated signaling inhibition in the context of MI-relevant DNA sensing and indicated that TF-FVIIa-PAR2

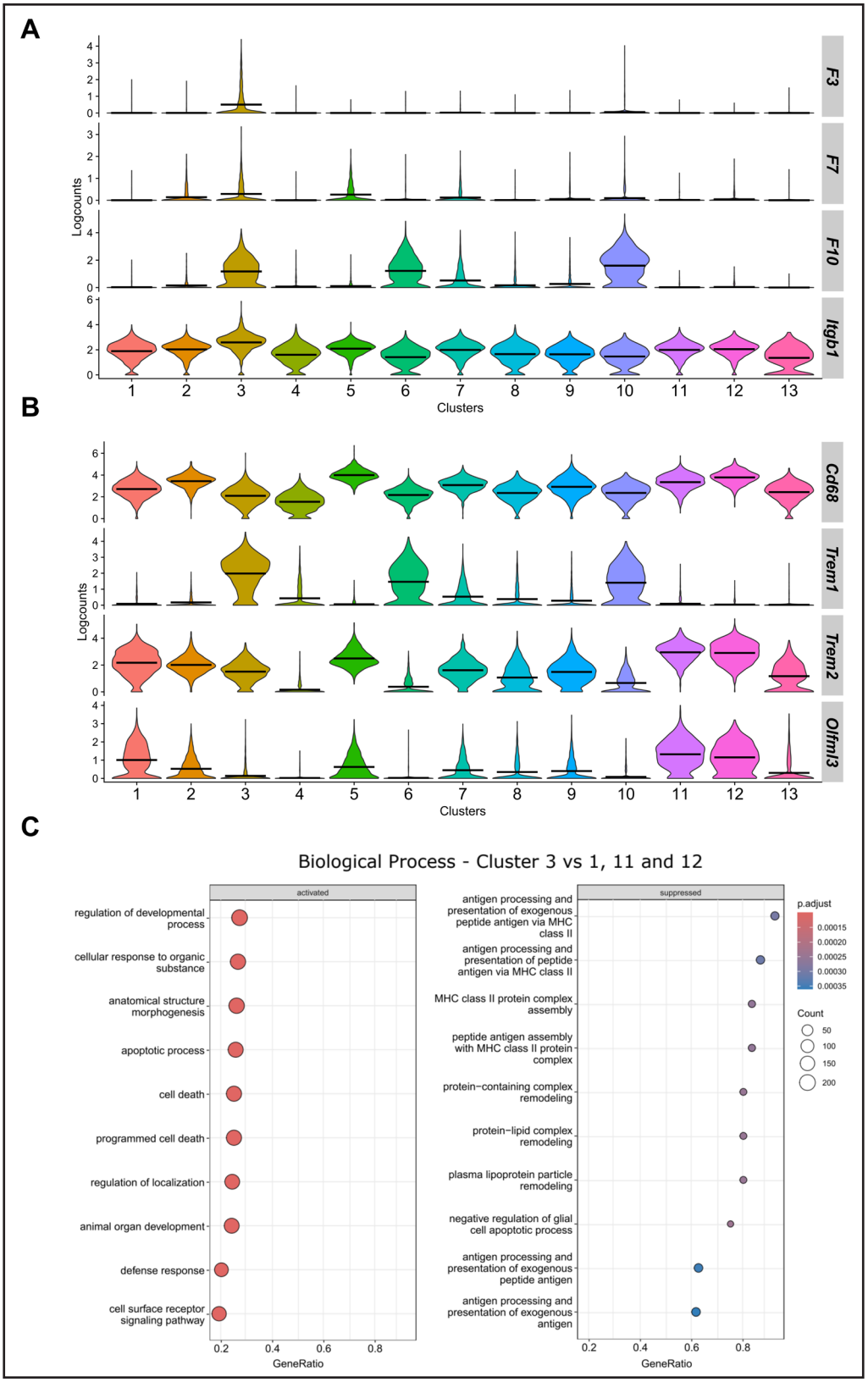

Figure 4. Characteristics of macrophage subsets in the infarcted myocardium.
Violin plots of log-transformed raw counts of (**A**) coagulation proteins tissue factor (TF; factor 3 [F3]), factor 7 (F7), and factor 10 (F10), as well as Itgb1, and (**B**) CD68 (cluster of differentiation 68), Trem1 (triggered receptor expressed on myeloid cells), Trem2, and Olfml (olfactomedin-like protein) 3. Note that clusters 1, 11, and 12 show a similar expression profile of Trem1, Trem2, and Olfml3. **C**, The top 1000 upregulated and top 1000 downregulated genes between cluster 3 and the combined clusters 1, 11, and 12 were used to determine differentially activated and repressed biological processes with clusterProfiler. The enrichment analysis revealed an inflammatory/apoptotic phenotype in cluster 3 vs clusters 1, 11, and 12. MHC indicates major histocompatibility complex.

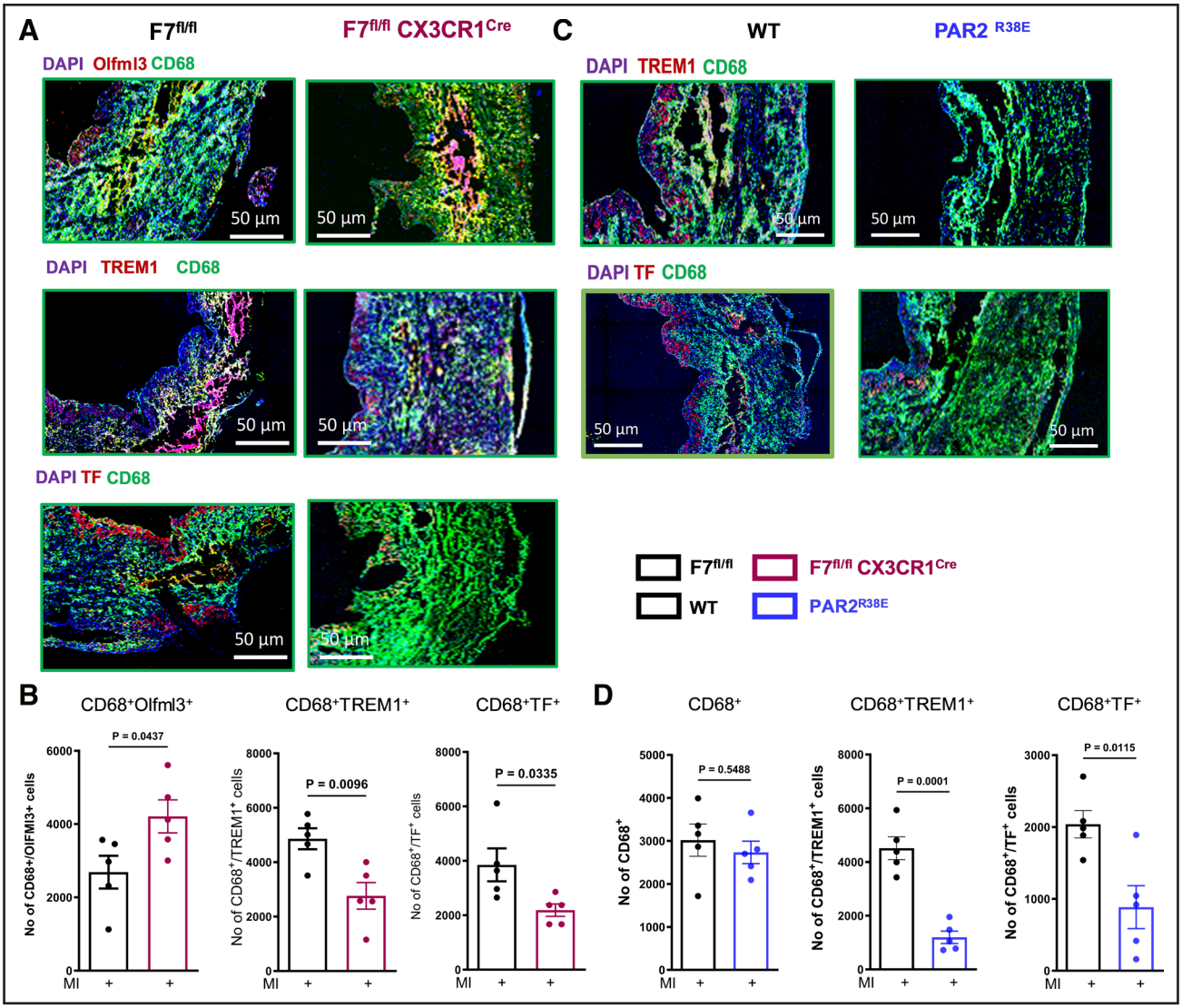

Figure 5. Localization and quantification of macrophage subsets in the infarcted myocardium 7 days after myocardial infarction (MI).

A, Representative confocal images of left ventricle infarct zones in myocardial cryo-sections obtained after 7 days post-MI. **B**, Quantification of CD68 (cluster of differentiation 68)$^{+}$Olfml (olfactomedin) 3^{+}, CD68^{+}TREM (triggered receptor expressed on myeloid cells) 1^{+}, and CD68^{+}tissue factor (TF)$^{+}$ cells in factor 7 (F7)$^{fl/fl}$ CX3CR1 (CX3C motif chemokine receptor 1)^{Cre} compared with F7$^{fl/fl}$ littermate mice. **C** and **D**, Representative confocal images and quantification of CD68^{+}TREM1^{+} and CD68^{+}TF^{+} cells in cleavage-resistant PAR2 (protease-activated receptor 2)^{R38E} compared with wild-type (WT) mice. All images were acquired with a 20× 0.75 NA dry objective with sequential scanning and detection for 4′,6-diamidino-2-phenylindole (DAPI; blue), Alexa Fluor 594 (CD68; green), and Alexa Fluor 647 (Olfml3, TREM1 and TF; red). Mean±SEM, n=5 animals/group, Welch unpaired *t* test.

signaling did not play a role in integrin β1-dependent macrophage migration, in line with the similar recruitment of monocyte/macrophages at day 3 post-MI in myeloid cell Itgb1- and F7-deficient mice.

To assess whether blockade of TF signaling without undesired effects on coagulation is sufficient for cardioprotection, we treated mice on days 1, 3, and 5 after LAD ligation with anti-TF 43D8 versus isotype-matched control IgG2a (Figure 6A). Specific inhibition of TF-FVIIa resulted in reduced dilation of the LV and improved left ventricular ejection fraction, starting at day 7 and persisting until day 28 post-MI (Figure 6B). This resulted in improved survival (Figure 6C) and reduced excess fibrotic remodeling of the LV (Figure 6D) 28 days post-MI. Consistently, systemic endothelial dysfunction as assessed by vascular relaxation studies of isolated aortic segments was impaired in ischemic heart failure mice with nonreperfused MI, while short-time intervention with anti-TF 43D8 in the first days after LAD ligation attenuated this phenotype (Figure 6E). Vascular inflammation after MI is a driver for endothelial dysfunction.[14] Treatment with anti-TF 43D8 decreased aortic mRNA levels of the myeloid cell–expressed pro-oxidant and inflammatory genes *NOX2*, *IL-1β*, and *MMP9* (Figure 6F),

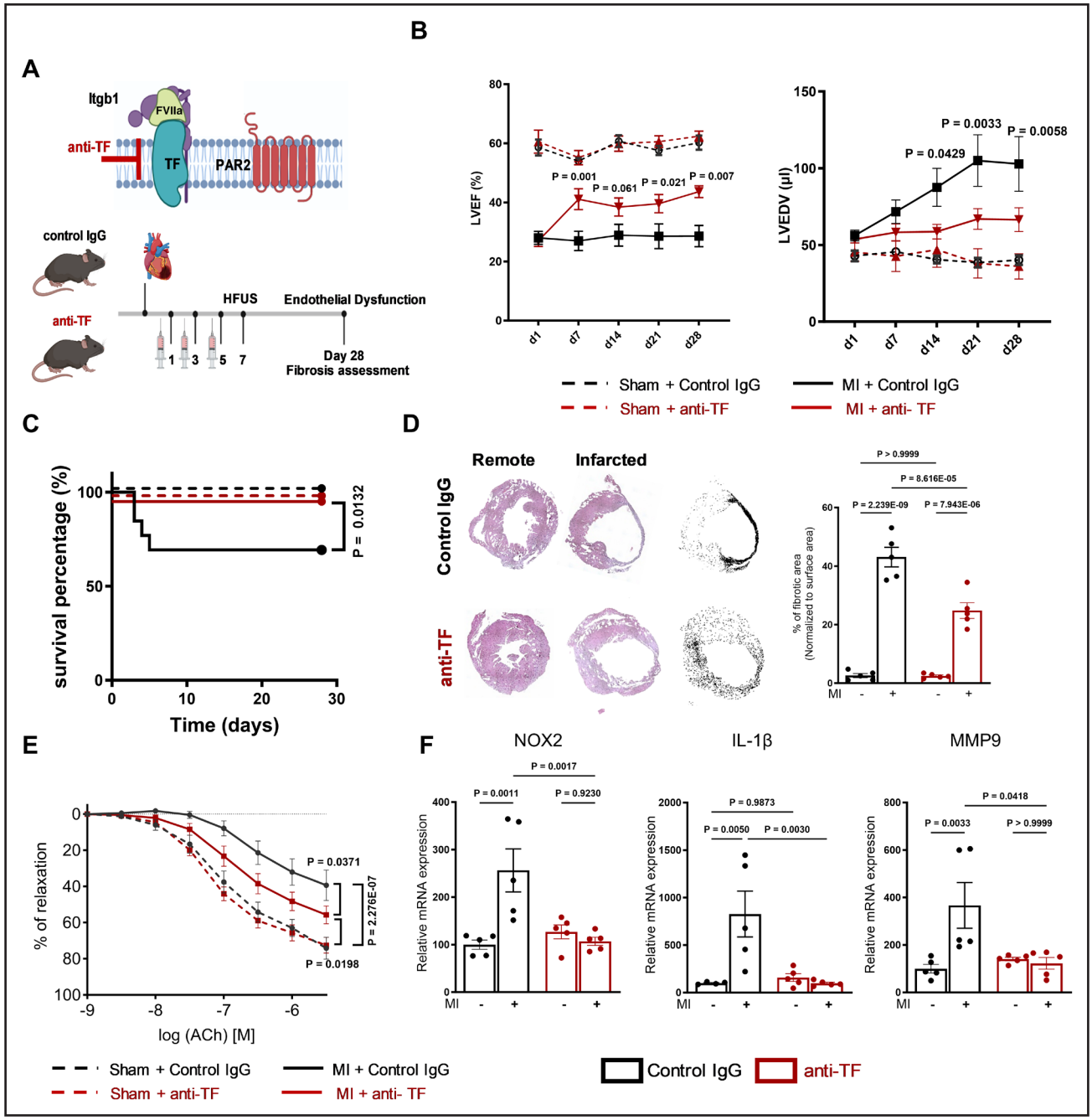

Figure 6. Pharmacological targeting the tissue factor (TF)-factor VIIa (FVIIa) signaling complex improved post-myocardial infarction (MI) recovery.

A, **Top**, Treatment scheme of mice with established MI received anti-TF 43D8 or control IgG (10 mg/kg) on days 1, 3, and 5. **B**, High-frequency echocardiography obtained in the parasternal long axis (PLAX) after left anterior descending artery (LAD) ligation and longitudinal echocardiography and quantification of left ventricular ejection fraction (LVEF) and left ventricular end diastolic volume (LVEDV) in the PLAX M-mode; n=6 to 10 animals/group, 2-way ANOVA, Tukey multiple comparison test. **C**, Kaplan-Meier survival analysis of LAD-ligated vs sham-operated mice treated with anti-TF and isotype control IgG, as shown in **A**; n=12 animals/group. **D**, Representative images and quantification of fibrotic areas normalized to total surface area in hearts from control or anti-TF–treated mice with sham surgery or LAD ligation 4 weeks earlier; n=5 animals/group, 1-way ANOVA, Sidak multiple comparison test. **E**, Endothelium-dependent (acetylcholine [Ach]) relaxation of thoracic aortic rings measured by isometric tension method. Aortas were obtained 4 weeks after sham surgery or LAD ligation with control IgG or anti-TF treatment; n=5 to 7 animals/group, 2-way ANOVA with Tukey multiple comparison test. **F**, mRNA expression analysis for NOX (nicotinamide adenine dinucleotide phosphate hydrogen oxidase) 2, IL (interleukin)-1β, and MMP (matrix metalloproteinase) 9 in aortic tissue obtained 4 weeks post-MI; mean±SEM, n=5 animals/group, 1-way ANOVA, Sidak multiple comparison test and Kruskal-Wallis test (MMP9). Scheme created with the help of *BioRender*.com.

indicating reduced vascular infiltration with immune cells in the aorta of anti-TF treated mice.[14]

Cardiovascular diseases have sex-specific differences in pathogenesis[29] and outcomes.[30] While the above experiments were performed in age-matched male mice, we affirmed the translational impact of the delineated mechanism by a pharmacological intervention study in females. Female LAD-ligated mice showed no increased lethality, consistent with published evidence[31] (Figure S12B). However, treatment with the inhibitory anti-mouse TF 43D8 partially preserved LV systolic function (Figure S12C) and prevented ischemic fibrotic remodeling to a similar extent as seen in males (Figure S11D). Post-MI vascular dysfunction was not increased in female mice, which also showed no evidence of increased vascular inflammation 28 days after MI[14] (Figure S12E and S12F). Thus, specific targeting of TF-FVIIa–dependent signaling has beneficial effects on post-MI remodeling, mitigates the development of ischemic heart failure in mice of both sexes, prevents systemic vascular dysfunction, and reduces mortality in male mice.

DISCUSSION

Inhibition of coagulation and platelet activation are established and effective therapeutic interventions in the prevention and treatment of ischemic heart disease. The hemostatic system and, particularly, the TF pathway also play pivotal roles in inflammation and tissue repair after injury. Specific therapeutic interventions targeting TF have to date not reached clinical applications due to concerns of increased bleeding risk. Here, we demonstrate a novel and specific role of macrophage-expressed FVII in adverse postischemic remodeling. We show that inhibition of the noncoagulant functions of the TF-FVIIa complex achieves a rebalancing of inflammation toward reparative macrophage functions following MI.

We had previously shown that inhibition of TF with recombinant NAPc2 (nematode anticoagulant protein c2) was effective in averting the development of ischemic heart failure in a preclinical model of nonreperfused MI by blocking the TF-PAR2/ERK/TGFβ1 signaling cascade.[6] Although NAPc2 inhibits the TF-FVIIa complex and its signaling function, this inhibitor also interferes with TF prothrombotic activities in a complex manner[32,33] and has multiple antithrombotic,[34,35] signaling, and immunemodulatory properties.[11,36] Using anti-TF 43D8 that has minimal antithrombotic properties but blocks TF-FVIIa-PAR2 dependent signaling, we here demonstrate a therapeutic window of opportunity in persisting myocardial ischemia to achieve beneficial myeloid cell reprogramming and improve long-term cardiovascular function. Without the risk of increased bleeding, this strategy protects from adverse cardiac remodeling after MI and may decrease the risk of ischemic heart failure.

Mechanistically, we show that the synthesis of FVII by monocyte/macrophages leads to the engagement of integrin β1 in the infarct zone and promotes PAR2 cleavage–dependent myocardial dysfunction. With single-cell sequencing–based monocyte/macrophage profiling, we identify a trajectory of differentiation from recruited monocytes to an integrin β1-TF-FVII expressing macrophage population with an inflammatory phenotype. In addition to the extrahepatic synthesis of FVII our data also reveal the expression of coagulation FX (encoded by F10 gene) in newly recruited monocytes on a path of differentiation toward macrophages. While FX expression rather declines in $TF^{+}FVII^{+}$ inflammatory macrophages, the expression of all components of the TF coagulation initiation complex in this detrimental cell population is in line with the previously demonstrated therapeutic efficacy of the FX-dependent inhibitor NAPc2. Moreover, our data show that specific blockade of TF-FVIIa dependent protease signaling is sufficient for beneficial reprogramming of cardiac macrophages and results in cardioprotection after MI.

There are multiple potential ligands that can engage with various integrin β1 heterodimers with diverse functions in leukocyte trafficking into but putatively also outside of inflamed tissue.[37] A specific integrin-binding site in the FVIIa protease domain enables complex formation with active integrin β1 and stimulates cell migration and PAR2 signaling leading to ERK1/2 activation.[8] The pharmacological antibody blockade of integrin β1-TF-FVIIa-PAR2 signaling did not impair macrophage migration on fibronectin, which is the extracellular matrix ligand for integrin α4/β1 and integrin α5/β1, in the context of DNA sensing, playing a pivotal role for macrophage polarization in myocardial ischemia.[28] These data are in line with the unaltered initial recruitment of integrin β1–deficient monocytes/macrophages and suggest that the specific interaction of FVIIa with integrins specifically affects the subsequent polarization to a proinflammatory macrophage at the expense of a reparative phenotype. Consequently, targeting the integrin β1-TF-FVIIa signaling effectively attenuated cardiac remodeling in nonreperfused MI and mitigated the development of ischemic heart failure both in male and female mice, in the absence of apparent bleeding complications.

Recently, several immune interventions have been evaluated to identify new therapeutic avenues for the treatment or prevention of ischemic heart failure. For example, TREM2 was found on a subset of macrophages with remodeling properties peaking 5 days post-MI, and injection of soluble TREM2 attenuates the development of heart failure in this setting.[2] In models of lung and liver fibrosis, $TREM2^{+}SPP1$ (secreted phosphoprotein 1)$^{+}$ macrophages are profibrotic and activated by TGF-ß1 for increased deposition of collagen type 1 and scarring.[38] In atherosclerosis, TREM2 plays a pivotal role in macrophage function, by regulating cholesterol efflux pathways

and reducing endoplasmic reticulum stress responses, which defines macrophage survival and effectively constrains plaque necrosis.[39,40]

Cardiac expression of TREM1 is increased after MI in mice, and levels of soluble TREM1 predict outcomes of MI patients.[41] Importantly, targeting TREM1 limits cardiac accumulation of neutrophils and inflammatory monocytes and protects from impaired cardiac function.[41] Our data implicate TREM1$^+$ monocyte-derived macrophages expressing the integrin β1 ligand fibronectin (FN1 [fibronectin 1]; Figure S4) in the adverse remodeling in cardiac ischemia. Mice with monocyte/macrophage F7 deficiency have decreased numbers of TREM1$^+$ macrophages, reduced ERK phosphorylation, and TGF-ß1 activation. These TREM1$^+$ cells are also Arg1 positive and resemble FN1 and osteopontin (SPP1) expressing macrophages associated with postischemic fibrotic tissue remodeling across organs and species, including heart failure.[42] SPP1 is an alternative ligand for integrin β1, regulated by platelet-derived CXCL4, and, thus, involves hemostatic-immune cell crosstalk. Similarly, SPP1$^+$ macrophages differentiate from recruited monocytes, accumulate in atrial myocardium, and cause tissue remodeling and arrhythmia in atrial fibrillation.[43] Our data indicate that an intracellular coagulation signaling mechanism drives polarization toward TREM1$^+$ macrophages as the culprits for the activation of myofibroblasts.[6]

TREM2 is more broadly expressed by macrophages in the infarcted myocardium than TREM1, supporting an important role as a decision maker in myeloid cell trajectories and in tissue (mal)adaptive responses to inflammatory stress.[42,43] In our study, TREM2 was predominantly upregulated in the repair type macrophage populations, which were expanded in monocyte/macrophage F7–deficient mice. These macrophages can be identified by the expression of Olfml3, which encodes the secreted extracellular matrix glycoprotein Olfml3 with a C-terminal olfactomedin domain mediating cell adhesion and intercellular interactions. Olfml3 is important for angiogenesis and is upregulated in macrophages after MI dependent on TGF-ß1.[44] The expansion of Olfml3$^+$CD68$^+$ macrophages in monocyte/macrophage F7 deficiency is, thus, consistent with the regenerative effect of macrophage reprogramming seen in our study.

In principle, activation of self-renewing and tissue-homeostatic properties of cardiac resident macrophages may confer cardioprotection after MI.[45] Yet, tissue-resident macrophages represent a minor cell population in our data set 7 days after acute MI. Our study clearly indicates that manipulating monocyte-derived macrophages, which represent the majority of accumulated immune cells post-MI,[1] is effective in inducing cardioprotection. Moreover, this reprogramming of monocyte-derived macrophages can be achieved by antagonizing a noncanonical signaling function of coagulation and is feasible to rebalance the inflammatory response post-MI. Thus, our strategy provides new therapeutic prospects to prevent and treat ischemic heart failure.

ARTICLE INFORMATION

Received December 6, 2023; revision received August 23, 2024; accepted August 25, 2024.

Affiliations

Center for Thrombosis and Hemostasis (V.G., Q.L., J.P., M.A., T.S.N., K.G., M.M., S.F., W.R., P.W.), Department of Cardiology (V.G., Q.L., M.A., M.M., S.F., P.W.), German Center for Cardiovascular Research-Partner site Rhine-Main (V.G., Q.L., M.A., M.M., W.R., P.W.), Institute of Immunology and Research Center for Immunotherapy (G.H., T.B.), and Cell Biology Unit (G.H.), University Medical Center Mainz, Germany. Department of Biochemistry, Cardiovascular Research Maastricht University, the Netherlands (Q.L.). Department of Biology, Wilkes University, Wilkes-Barre, PA (G.H.). Department of Immunology and Microbiology, Scripps Research, La Jolla, CA (W.R.).

Acknowledgments

The authors thank Katharina Perius and Petra Wilgenbus for their expert technical assistance.

Author Contributions

V. Garlapati designed and performed experiments, analyzed data, and prepared the article draft. Q. Luo performed experiments and analyzed data. J. Posma performed the bioinformatics analysis. M. Aluia, T.S. Nguyen, K. Grunz, M. Molitor, and S. Finger jointly performed experiments and assisted in experimental design and analysis. G. Harms assisted in designing, conducting, and analyzing imaging experiments. T. Bopp provided assistance in experimental design and writing. W. Ruf conceptualized experiments, provided intellectual input, discussed results and strategy, and wrote the article. P. Wenzel conceptualized, coordinated, and supervised the study, interpreted experiments, provided intellectual input and results discussion, and wrote the article.

Sources of Funding

This work was supported by the Deutsche Stiftung für Herzforschung (grant F/09/21), the Clusters for Future grant curATime (BMBF [Bundesministerium für Bildung und Forschung] grants 03ZU1202HA and 03ZU1202BA), and the German Research Foundation for Large Instrumentation Grant (DFG INST 371/47-1 FUGG). Q. Luo was supported by the European Union's Horizon 2020 Research and Innovation Program under the Marie Sklodowska-Curie grant Agreement TICARDIO No. 813409. M. Molitor was supported by the German Center for Cardiovascular Research (grant FKZ 81X3210105), the Centre for Healthy Ageing Programme for Clinician Scientists (CHANCE) of the Center for Healthy Aging Mainz, and the Else Kroner-Fresenius Foundation (grant 2021_2020_EKEA.144). G. Harms acknowledges continued funding for the Research Center for Immunotherapy and the Cell Biology Unit, University Medical Center Mainz, Germany. P. Wenzel was supported by the German Research Foundation (grant DFG WE WE4361/14-1) and the Boehringer Ingelheim Foundation. W. Ruf received funding from the Alexander von Humboldt Foundation, the Boehringer Ingelheim Foundation, the German Research Foundation (project numbers 318346496 and SFB1292/2 TP02), and Endpoint Health.

Disclosures

W. Ruf is a consultant and received research support from Endpoint Health. W. Ruf and P. Wenzel have filed a patent application on the use of inhibitors of the tissue factor (TF)-PAR2 (protease activated receptor 2) signaling for the treatment or prevention of heart failure (PCT/EP2021/082355). The other authors report no conflicts.

REFERENCES

1. Swirski FK, Nahrendorf M. Cardioimmunology: the immune system in cardiac homeostasis and disease. *Nat Rev Immunol.* 2018;18:733–744. doi: 10.1038/s41577-018-0065-8
2. Jung SH, Hwang BH, Shin S, Park EH, Park SH, Kim CW, Kim E, Choo E, Choi IJ, Swirski FK, et al. Spatiotemporal dynamics of macrophage heterogeneity and a potential function of TREM2(hi) macrophages in infarcted hearts. *Nat Commun.* 2022;13:4580. doi: 10.1038/s41467-022-32284-2
3. Rizzo G, Gropper J, Piollet M, Vafadarnejad E, Rizakou A, Bandi SR, Arampatzi P, Krammer T, DiFabion N, Dietrich O, et al. Dynamics of monocyte-derived

macrophage diversity in experimental myocardial infarction. *Cardiovasc Res*. 2023;119:772–785. doi: 10.1093/cvr/cvac113
4. Skelly DA, Squiers GT, McLellan MA, Bolisetty MT, Robson P, Rosenthal NA, Pinto AR. Single-cell transcriptional profiling reveals cellular diversity and intercommunication in the mouse heart. *Cell Rep*. 2018;22:600–610. doi: 10.1016/j.celrep.2017.12.072
5. Zhang K, Wang Y, Chen S, Mao J, Jin Y, Ye H, Zhang Y, Liu X, Gong C, Cheng X, et al. TREM2(hi) resident macrophages protect the septic heart by maintaining cardiomyocyte homeostasis. *Nat Metab*. 2023;5:129–146. doi: 10.1038/s42255-022-00715-5
6. Garlapati V, Molitor M, Michna T, Harms GS, Finger S, Jung R, Lagrange J, Efentakis P, Wild J, Knorr M, et al. Targeting myeloid cell coagulation signaling blocks MAP kinase/TGF-beta1-driven fibrotic remodeling in ischemic heart failure. *J Clin Invest*. 2023;133:e156436. doi: 10.1172/JCI156436
7. Muller-Calleja N, Hollerbach A, Ritter S, Pedrosa DG, Strand D, Graf C, Reinhardt C, Strand S, Poncelet P, Griffin JH, et al. Tissue factor pathway inhibitor primes monocytes for antiphospholipid antibody-induced thrombosis. *Blood*. 2019;134:1119–1131. doi: 10.1182/blood.2019001530
8. Rothmeier AS, Liu E, Chakrabarty S, Disse J, Mueller BM, Østergaard H, Ruf W. Identification of the integrin-binding site on coagulation factor VIIa required for proangiogenic PAR2 signaling. *Blood*. 2018;131:674–685. doi: 10.1182/blood-2017-02-768218
9. Zelaya H, Grunz K, Nguyen TS, Habibi A, Witzler C, Reyda S, Gonzalez-Menendez I, Quintanilla-Martinez L, Bosmann M, Weiler H, et al. Nucleic acid sensing promotes inflammatory monocyte migration through biased coagulation factor VIIa signaling. *Blood*. 2024;143:845–857. doi: 10.1182/blood.2023021149
10. Saffarzadeh M, Grunz K, Nguyen TS, Lee YK, Kitano M, Danckwardt S, Rodrigues CDS, Weiler H, Reyda S, Ruf W. Macrophage protease-activated receptor 2 regulates fetal liver erythropoiesis in mice. *Blood Adv*. 2020;4:5810–5824. doi: 10.1182/bloodadvances.2020003299
11. Liang HP, Kerschen EJ, Hernandez I, Basu S, Zogg M, Botros F, Jia S, Hessner MJ, Griffin JH, Ruf W, et al. EPCR-dependent PAR2 activation by the blood coagulation initiation complex regulates LPS-triggered interferon responses in mice. *Blood*. 2015;125:2845–2854. doi: 10.1182/blood-2014-11-610717
12. Fleischer MI, Rohrig N, Raker VK, Springer J, Becker D, Ritz S, Bros M, Stege H, Haist M, Grabbe S, et al. Protease- and cell type-specific activation of protease-activated receptor 2 in cutaneous inflammation. *J Thromb Haemost*. 2022;20:2823–2836. doi: 10.1111/jth.15894
13. Yona S, Kim KW, Wolf Y, Mildner A, Varol D, Breker M, Strauss-Ayali D, Viukov S, Guilliams M, Misharin A, et al. Fate mapping reveals origins and dynamics of monocytes and tissue macrophages under homeostasis. *Immunity*. 2013;38:79–91. doi: 10.1016/j.immuni.2012.12.001
14. Molitor M, Rudi WS, Garlapati V, Finger S, Schuler R, Kossmann S, Lagrange J, Nguyen TS, Wild J, Knopp T, et al. Nox2^{+} myeloid cells drive vascular inflammation and endothelial dysfunction in heart failure after myocardial infarction via angiotensin ii receptor type 1. *Cardiovasc Res*. 2021;117:162–177. doi: 10.1093/cvr/cvaa042
15. McCarthy DJ, Campbell KR, Lun AT, Wills QF. Scater: pre-processing, quality control, normalization and visualization of single-cell RNA-seq data in R. *Bioinformatics*. 2017;33:1179–1186. doi: 10.1093/bioinformatics/btw777
16. Lun AT, McCarthy DJ, Marioni JC. A step-by-step workflow for low-level analysis of single-cell RNA-seq data with bioconductor. *F1000Res*. 2016;5:2122. doi: 10.12688/f1000research.9501.2
17. Germain PL, Lun A, Garcia Meixide C, Macnair W, Robinson MD. Doublet identification in single-cell sequencing data using *scDblFinder*. *F1000Res*. 2021;10:979. doi: 10.12688/f1000research.73600.2
18. Vafadarnejad E, Rizzo G, Krampert L, Arampatzi P, Arias-Loza AP, Nazzal Y, Rizakou A, Knochenhauer T, Bandi SR, Nugroho VA, et al. Dynamics of cardiac neutrophil diversity in murine myocardial infarction. *Circ Res*. 2020;127:e232–e249. doi: 10.1161/CIRCRESAHA.120.317200
19. Haghverdi L, Lun ATL, Morgan MD, Marioni JC. Batch effects in single-cell RNA-sequencing data are corrected by matching mutual nearest neighbors. *Nat Biotechnol*. 2018;36:421–427. doi: 10.1038/nbt.4091
20. Aran D, Looney AP, Liu L, Wu E, Fong V, Hsu A, Chak S, Naikawadi RP, Wolters PJ, Abate AR, et al. Reference-based analysis of lung single-cell sequencing reveals a transitional profibrotic macrophage. *Nat Immunol*. 2019;20:163–172. doi: 10.1038/s41590-018-0276-y
21. Hao Y, Hao S, Andersen-Nissen E, Mauck WM 3rd, Zheng S, Butler A, Lee MJ, Wilk AJ, Darby C, Zager M, et al. Integrated analysis of multimodal single-cell data. *Cell*. 2021;184:3573–3587.e29. doi: 10.1016/j.cell.2021.04.048
22. Rothmeier AS, Marchese P, Petrich BG, Furlan-Freguia C, Ginsberg MH, Ruggeri ZM, Ruf W. Caspase-1-mediated pathway promotes generation of thromboinflammatory microparticles. *J Clin Invest*. 2015;125:1471–1484. doi: 10.1172/JCI79329
23. Schindelin J, Arganda-Carreras I, Frise E, Kaynig V, Longair M, Pietzsch T, Preibisch S, Rueden C, Saalfeld S, Schmid B, et al. Fiji: an open-source platform for biological-image analysis. *Nat Methods*. 2012;9:676–682. doi: 10.1038/nmeth.2019
24. Bankhead P, Loughrey MB, Fernández JA, Dombrowski Y, McArt DG, Dunne PD, McQuaid S, Gray RT, Murray LJ, Coleman HG, et al. Qupath: open source software for digital pathology image analysis. *Sci Rep*. 2017;7:16878. doi: 10.1038/s41598-017-17204-5
25. Kossmann S, Lagrange J, Jackel S, Jurk K, Ehlken M, Schonfelder T, Weihert Y, Knorr M, Brandt M, Xia N, et al. Platelet-localized FXI promotes a vascular coagulation-inflammatory circuit in arterial hypertension. *Sci Transl Med*. 2017;9:eaah4923. doi: 10.1126/scitranslmed.aah4923
26. Chapman HA Jr, Allen CL, Stone OL, Fair DS. Human alveolar macrophages synthesize factor vii in vitro. Possible role in interstitial lung disease. *J Clin Invest*. 1985;75:2030–2037. doi: 10.1172/JCI111922
27. Gautier EL, Shay T, Miller J, Greter M, Jakubzick C, Ivanov S, Helft J, Chow A, Elpek KG, Gordonov S, et al; Immunological Genome Consortium. Gene-expression profiles and transcriptional regulatory pathways that underlie the identity and diversity of mouse tissue macrophages. *Nat Immunol*. 2012;13:1118–1128. doi: 10.1038/ni.2419
28. Cao DJ, Schiattarella GG, Villalobos E, Jiang N, May HI, Li T, Chen ZJ, Gillette TG, Hill JA. Cytosolic DNA sensing promotes macrophage transformation and governs myocardial ischemic injury. *Circulation*. 2018;137:2613–2634. doi: 10.1161/CIRCULATIONAHA.117.031046
29. Shufelt CL, Pacheco C, Tweet MS, Miller VM. Sex-specific physiology and cardiovascular disease. *Adv Exp Med Biol*. 2018;1065:433–454. doi: 10.1007/978-3-319-77932-4_27
30. SCORE2 Working Group and ESC Cardiovascular Risk Collaboration. Score2 risk prediction algorithms: new models to estimate 10-year risk of cardiovascular disease in Europe. *Eur Heart J*. 2021;42:2439–2454. doi: 10.1093/eurheartj/ehab309
31. Cavasin MA, Tao Z, Menon S, Yang XP. Gender differences in cardiac function during early remodeling after acute myocardial infarction in mice. *Life Sci*. 2004;75:2181–2192. doi: 10.1016/j.lfs.2004.04.024
32. Bergum PW, Cruikshank A, Maki SL, Kelly CR, Ruf W, Vlasuk GP. Role of zymogen and activated factor x as scaffolds for the inhibition of the blood coagulation factor VIIa-tissue factor complex by recombinant nematode anticoagulant protein c2. *J Biol Chem*. 2001;276:10063–10071. doi: 10.1074/jbc.M009116200
33. Kamikubo Y, Mendolicchio GL, Zampolli A, Marchese P, Rothmeier AS, Nagrampa Orje J, Gale AJ, Krishnaswamy S, Gruber A, Ostergaard H, et al. Selective factor VIII activation by the tissue factor-factor VIIa-factor Xa complex. *Blood*. 2017;130:1661–1670. doi: 10.1182/blood-2017-02-767079
34. Hess CN, Hsia J, Carroll IA, Nehler MR, Ruf W, Morrow DA, Nicolau JC, Berwanger O, Szarek M, Capell WH, et al. Novel tissue factor inhibition for thromboprophylaxis in covid-19: primary results of the aspen-covid-19 trial. *Arterioscler Thromb Vasc Biol*. 2023;43:1572–1582. doi: 10.1161/ATVBAHA.122.318748
35. Lee A, Agnelli G, Buller H, Ginsberg J, Heit J, Rote W, Vlasuk G, Costantini L, Julian J, Comp P, et al. Dose-response study of recombinant factor VIIa/tissue factor inhibitor recombinant nematode anticoagulant protein c2 in prevention of postoperative venous thromboembolism in patients undergoing total knee replacement. *Circulation*. 2001;104:74–78. doi: 10.1161/hc2601.091386
36. Grover SP, Mackman N. Tissue factor: an essential mediator of hemostasis and trigger of thrombosis. *Arterioscler Thromb Vasc Biol*. 2018;38:709–725. doi: 10.1161/ATVBAHA.117.309846
37. Barkaway A, Rolas L, Joulia R, Bodkin J, Lenn T, Owen-Woods C, Reglero-Real N, Stein M, Vazquez-Martinez L, Girbl T, et al. Age-related changes in the local milieu of inflamed tissues cause aberrant neutrophil trafficking and subsequent remote organ damage. *Immunity*. 2021;54:1494–1510 e1497. doi: 10.1016/j.immuni.2021.04.025
38. Fabre T, Barron AMS, Christensen SM, Asano S, Bound K, Lech MP, Wadsworth MH 2nd, Chen X, Wang C, Wang J, et al. Identification of a broadly fibrogenic macrophage subset induced by type 3 inflammation. *Sci Immunol*. 2023;8:eadd8945. doi: 10.1126/sciimmunol.add8945
39. Piollet M, Porsch F, Rizzo G, Kapser F, Schulz DJJ, Kiss MG, Schlepckow K, Morenas-Rodriguez E, Sen MO, Gropper J, et al. Trem2 limits necrotic core formation during atherogenesis by controlling macrophage survival and efferocytosis. *bioArxiv*. 2023;3:269. doi: 10.1038/s44161-024-00429-9
40. Patterson MT, Firulyova MM, Xu Y, Hillman H, Bishop C, Zhu A, Hickok GH, Schrank PR, Ronayne CE, Caillot Z, et al. Trem2 promotes

foamy macrophage lipid uptake and survival in atherosclerosis. *Nat Cardiovasc Res*. 2023;2:1015–1031. doi: 10.1038/s44161-023-00354-3
41. Boufenzer A, Lemarie J, Simon T, Derive M, Bouazza Y, Tran N, Maskali F, Groubatch F, Bonnin P, Bastien C, et al. Trem-1 mediates inflammatory injury and cardiac remodeling following myocardial infarction. *Circ Res*. 2015;116:1772–1782. doi: 10.1161/CIRCRESAHA.116.305628
42. Hoeft K, Schaefer GJL, Kim H, Schumacher D, Bleckwehl T, Long Q, Klinkhammer BM, Peisker F, Koch L, Nagai J, et al. Platelet-instructed spp1^{+} macrophages drive myofibroblast activation in fibrosis in a cxcl4-dependent manner. *Cell Rep*. 2023;42:112131. doi: 10.1016/j.celrep.2023.112131
43. Hulsmans M, Schloss MJ, Lee IH, Bapat A, Iwamoto Y, Vinegoni C, Paccalet A, Yamazoe M, Grune J, Pabel S, et al. Recruited macrophages elicit atrial fibrillation. *Science*. 2023;381:231–239. doi: 10.1126/science.abq3061
44. Li J, Li R, Tuleta I, Hernandez SC, Humeres C, Hanna A, Chen B, Frangogiannis NG. The role of endogenous smad7 in regulating macrophage phenotype following myocardial infarction. *FASEB J*. 2022;36:e22400. doi: 10.1096/fj.202101956RR
45. Dick SA, Macklin JA, Nejat S, Momen A, Clemente-Casares X, Althagafi MG, Chen J, Kantores C, Hosseinzadeh S, Aronoff L, et al. Self-renewing resident cardiac macrophages limit adverse remodeling following myocardial infarction. *Nat Immunol*. 2019;20:29–39. doi: 10.1038/s41590-018-0272-2